

1
2
3
4
5
6
7
8
9
10
11
12
13
14
15
16
17
18
19
20

Bacterial biodiversity drives the evolution of CRISPR-based phage resistance in *Pseudomonas aeruginosa*

Ellinor O Alseth^{1*}, Elizabeth Pursey¹, Adela M Luján², Isobel McLeod¹, Clare Rollie¹, Edze R Westra^{1*}

¹*Environmental and Sustainability Institute, Biosciences, University of Exeter,*

Cornwall Campus, Penryn, Cornwall TR10 9FE, United Kingdom

²*IRNASUS, CONICET, Facultad de Ciencias Químicas, Universidad Católica de Córdoba,*

Avda. Armada Argentina 3555, X5016DHK, Córdoba, Argentina

*Correspondence: E.R.Westra@exeter.ac.uk, eao210@exeter.ac.uk

Keywords: CRISPR-Cas; *Pseudomonas aeruginosa*; cystic fibrosis; fitness trade-offs; evolution of virulence; biodiversity

21

22 **Approximately half of all bacterial species encode CRISPR-Cas adaptive immune**
23 **systems¹, which provide immunological memory by inserting short DNA sequences**
24 **from phage and other parasitic DNA elements into CRISPR loci on the host genome².**
25 **Whereas CRISPR loci evolve rapidly in natural environments³, bacterial species**
26 **typically evolve phage resistance by the mutation or loss of phage receptors under**
27 **laboratory conditions^{4,5}. Here, we report how this discrepancy may in part be explained**
28 **by differences in the biotic complexity of *in vitro* and natural environments^{6,7}.**
29 **Specifically, using the opportunistic pathogen *Pseudomonas aeruginosa* and its phage**
30 **DMS3*vir*, we show that coexistence with other human pathogens amplifies the fitness**
31 **trade-offs associated with phage receptor mutation, and therefore tips the balance in**
32 **favour of CRISPR-based resistance evolution. We also demonstrate that this has**
33 **important knock-on effects for *P. aeruginosa* virulence, which became attenuated only if**
34 **the bacteria evolved surface-based resistance. Our data reveal that the biotic complexity**
35 **of microbial communities in natural environments is an important driver of the**
36 **evolution of CRISPR-Cas adaptive immunity, with key implications for bacterial fitness**
37 **and virulence.**

38

39 *Pseudomonas aeruginosa* is a widespread opportunistic human pathogen that thrives in a
40 range of different environments, including hospitals, where it is a common source of
41 nosocomial infections. In particular, it frequently colonises the lungs of cystic fibrosis
42 patients, in whom it is the leading cause of morbidity and mortality⁸. In part fuelled by a
43 renewed interest in the therapeutic use of bacteriophages as antimicrobials (phage
44 therapy)^{9,10}, many studies have examined if and how *P. aeruginosa* evolves resistance to
45 phage (reviewed in ref. 11). The clinical isolate *P. aeruginosa* strain PA14 has been reported
46 to predominantly evolve resistance against its phage DMS3*vir* by the modification or
47 complete loss of the phage surface receptor¹² when grown in nutrient-rich medium⁴ despite
48 carrying an active CRISPR-Cas adaptive immune system (Clustered Regularly Interspaced
49 Short Palindromic Repeats; CRISPR-associated). Conversely, under nutrient-limited
50 conditions, the same strain relies on CRISPR-Cas to acquire phage resistance⁴. While these
51 observations suggest abiotic factors are critical determinants of the evolution of phage
52 resistance strategies, the role of biotic factors has remained unclear, even though *P.*
53 *aeruginosa* commonly co-exists with a range of other bacterial species in both natural and
54 clinical settings^{13,14}.

55 To explore how microbial biodiversity impacts the evolution of phage resistance, we
56 co-cultured *P. aeruginosa* PA14 with three other clinically relevant opportunistic pathogens
57 that are known to co-infect with *P. aeruginosa*, namely *Staphylococcus aureus*, *Burkholderia*
58 *cenocepacia*, and *Acinetobacter baumannii*¹⁴⁻¹⁶, none of which can be infected by or interact
59 with phage DMS3vir (Extended Data Fig. 1, Linear model: Effect of *P. aeruginosa* on phage
60 titre over time; $t = -3.37$, $p < 0.001$; *S. aureus*; $t = 1.63$, $p = 0.11$; *A. baumannii*; $t = 1.20$, $p =$
61 0.23 ; *B. cenocepacia*; $t = -0.27$, $p = 0.79$; Overall model fit; $F_{9,235} = 4.33$, adjusted $R^2 = 0.11$,
62 $p < 0.001$). We applied a “mark-recapture” approach using a *P. aeruginosa* PA14 mutant
63 carrying streptomycin resistance in order to monitor the bacterial population dynamics and
64 phage resistance evolution in the focal subpopulation at 3 days post infection (d.p.i.). This
65 revealed that in nutrient-rich broth (Lysogeny Broth), PA14 evolved significantly higher
66 levels of CRISPR-based resistance following infection with 10^6 plaque forming units (p.f.u.)
67 of phage DMS3vir when co-cultured with other bacterial species compared to when grown in
68 isolation or co-cultured with an isogenic surface mutant (Fig. 1). Additionally, we found that
69 these effects were dependent on the identity of the species that were present in the mixed
70 culture, with the strongest effects being observed in the presence of *A. baumannii* or a mix of
71 the three bacterial species, and an absence of any effect when PA14 was co-cultured with an
72 isogenic surface mutant that lacked the phage receptor (Fig. 1, Deviance test: Relationship
73 between community composition and CRISPR; Residual deviance(30, $n = 36$) = 1.81, $p <$
74 0.001 ; Tukey contrasts: Monoculture v Mixed; $z = -5.99$, $p < 0.001$; Monoculture v *A.*
75 *baumannii*; $z = -4.33$, $p < 0.001$; Monoculture v *B. cenocepacia*; $z = -3.76$, $p < 0.01$;
76 Monoculture v *S. aureus*; $z = -2.38$, $p = 0.14$; Monoculture v surface mutant; $z = 2.26$, $p =$
77 0.19). To explore the clinical relevance of this observation, we next co-cultured *P.*
78 *aeruginosa* with *A. baumannii* in artificial sputum medium (ASM), which mimics the abiotic
79 environment of sputum from cystic fibrosis patients¹⁷. This analysis revealed a similar effect
80 of *A. baumannii* on the evolution of CRISPR-based resistance in both LB and ASM
81 (Extended Data Fig. 2, Deviance test: Relationship between community composition and
82 CRISPR; Residual deviance(20, $n = 22$) = 2.33, $p < 0.001$; Relationship between growth
83 medium and CRISPR; Residual deviance(19, $n = 22$) = 2.30, $p = 0.59$). To further explore the
84 generality of our finding, we next manipulated the microbial community composition by
85 varying the proportion of *P. aeruginosa* versus the other pathogens. This revealed that
86 increased CRISPR-based resistance evolution occurred across a wide range of microbial
87 community compositions, with a maximum effect size when *P. aeruginosa* made up 50% of
88 the initial bacterial mixture (Extended Data Fig. 3). An exception to this trend was when the

89 *P. aeruginosa* subpopulation made up only 1% of the total community; in this case sensitive
90 bacteria persisted due to the reduced size of the phage epidemic and hence relaxed selection
91 for resistance (Extended Data Fig. 3). Collectively, these data suggest that greater levels of
92 interspecific competition contribute to the evolution of CRISPR-based resistance.

93 Given that cell surface molecules likely play a part in interspecific competition¹⁸, we
94 hypothesised that the fitness cost of surface-based resistance may be amplified in the
95 presence of other bacterial species, resulting in stronger selection for bacteria with CRISPR-
96 based resistance. To test this, we competed the two phage resistant phenotypes (i.e. CRISPR-
97 resistant and surface mutant clones) in the presence or absence of the microbial community,
98 and across a range of phage titres. In the absence of the microbial community and phage,
99 CRISPR-resistant bacteria showed a small fitness advantage over bacteria with surface-based
100 resistance, but this advantage disappeared when phage was added and as titres increased (Fig.
101 2a, and ref. 7). In the presence of the biodiverse microbial community however, the relative
102 fitness of bacteria with CRISPR-based resistance was consistently higher, demonstrating that
103 mutation of the Type IV pilus is more costly when bacteria compete with other bacterial
104 species (Fig. 2a, Linear model: Effect of community absence; $t = -5.54$, $p < 0.001$; Effect of
105 increasing phage titre; $t = -2.41$, $p < 0.05$; Overall model fit; Adjusted $R^2 = 0.41$, $F_{4,139} =$
106 25.48 , $p < 0.001$). This increased fitness trade-off associated with surface-based resistance
107 was also observed when the CRISPR- and surface-resistant phenotypes competed in the
108 presence of only a single additional species (Fig. 2b, ANOVA with Tukey contrasts: Overall
109 difference in fitness; $F_{4,2} = 8.151$ $p < 0.001$; Monoculture v Mixed; $p < 0.05$; Monoculture v
110 *A. baumannii*; $p < 0.05$; Monoculture v *B. cenocepacia*; $p < 0.05$), with the exception of *S.*
111 *aureus* (Fig. 2d. Monoculture v *S. aureus*; $p = 0.80$), concordant with this species inducing
112 the lowest levels of CRISPR (Fig. 1). These fitness trade-offs therefore explain why *P.*
113 *aeruginosa* evolved greater levels of CRISPR-based resistance in the presence of the other
114 pathogens, and why this varied depending on the species (Fig. 1).

115 Evolution of phage resistance by bacterial pathogens is often associated with
116 virulence trade-offs when surface structures are modified^{19–21}, whereas similar trade-offs
117 have not yet been reported in the literature for CRISPR-based resistance. We therefore
118 hypothesised that the community context in which phage resistance evolves may have
119 important knock-on effects for *P. aeruginosa* virulence. To test this, we used a *Galleria*
120 *mellonella* larvae infection model, which is commonly used to evaluate the virulence of
121 human pathogens^{22,23}. We compared *in vivo* virulence of *P. aeruginosa* clones that evolved
122 phage resistance in different community contexts by injecting larvae with a mixture of clones

123 that had evolved phage-resistance in either the presence or absence of the mixed bacterial
124 community (Extended Data Fig. 2). Taking time to death as a proxy for virulence, we found
125 that the evolution of phage resistance in the presence of a microbial community was
126 associated with greater levels of *P. aeruginosa* virulence compared to when phage-resistance
127 evolved in monoculture, and similar to that of the ancestral PA14 strain (Fig. 3a, Cox
128 proportional hazards model with Tukey contrasts: Community present v absent; $z = 5.85$, $p <$
129 0.001 ; ancestral PA14 v community absent; $z = 4.42$, $p < 0.001$; ancestral PA14 v community
130 present; $z = -1.30$, $p = 0.38$. Overall model fit; $LRT_3 = 51.03$, $n = 376$, $p < 0.001$). These data,
131 in combination with the fact that the Type IV pilus is a well-known virulence factor^{19,24}, are
132 consistent with the idea that the mechanism by which bacteria evolve phage resistance has
133 important implications for bacterial virulence. To more directly test this, we next infected
134 larvae with each individual *P. aeruginosa* clone for which we had previously determined the
135 mechanism underlying evolved phage resistance (Extended Data Fig. 2), again using time to
136 death as a measure of virulence. This showed that bacterial clones with surface-based
137 resistance both had drastically reduced swarming motility (consistent with mutations in the
138 Type IV pilus¹⁹) (Fig. 3b, ANOVA with Tukey contrasts: Overall effect; $F_{2,977} = 472.5$, $p <$
139 0.001 ; Sensitive v CRISPR; $p = 0.88$; CRISPR v Surface mutant ; $p < 0.001$) and impaired
140 virulence (Fig. 3c, Cox proportional hazards model with Tukey contrasts: Surface mutant v
141 CRISPR; $z = -2.37$, $p < 0.05$; Sensitive v CRISPR; $z = 2.10$, $p = 0.10$; Surface mutant v
142 Sensitive; $z = -4.23$, $p < 0.001$. Overall model fit; $LRT_3 = 48.66$, $n = 981$, $p < 0.001$).

143 Collectively, our data show that the evolutionary outcome of bacteria-phage
144 interactions can be fundamentally altered by the microbial community context. While
145 traditionally studied in isolation, these interactions are usually embedded in complex biotic
146 networks of multiple species, and it is becoming increasingly clear that this can have key
147 implications for the evolutionary epidemiology of infectious disease, including the evolution
148 of pathogen virulence and host range²⁵⁻²⁹. The work presented here reveals that the
149 community context can also shape the evolution of different host resistance strategies.
150 Specifically, we find that the interspecific interactions between four bacterial species in a
151 synthetic microbial community can have a large impact on the evolution of phage resistance
152 mechanisms by amplifying the constitutive fitness cost of surface-based resistance⁴. The
153 finding that biotic complexity matters complements previous work on the effect of abiotic
154 variables on phage resistance evolution. This previous work showed that a greater force of
155 infection resulted in a higher induced fitness cost of CRISPR-based resistance, hence
156 selecting for surface-based resistance in the presence of higher phage titres⁴. Variation in the

157 force of infection did not however seem to play a role in the effects described in this study,
158 since even though phage epidemic sizes varied depending on the microbial community
159 composition (Extended Data Fig. 4, ANOVA: Overall effect of *P. aeruginosa* starting
160 percentage on phage titre; $F_{6,105} = 14.84$, $p < 0.001$), they did not correlate with the levels of
161 evolved CRISPR-based resistance (Extended Data Fig. 5). This therefore suggests that in this
162 case the impact of biotic complexity on the evolution of CRISPR-based resistance is stronger
163 than that of variation in phage abundance. While future work will be critical to further
164 generalise the findings described here to other bacterial species and strains, we speculate that
165 the way in which the microbial community composition drives the evolution of phage
166 resistance strategies may be important in the context of phage therapy. Primarily, the absence
167 of detectable trade-offs between CRISPR-based resistance and virulence, as opposed to when
168 bacteria evolve surface-based resistance, suggests that evolution of CRISPR-based resistance
169 can ultimately influence the severity of disease. Moreover, evolution of CRISPR-based
170 resistance can drive more rapid phage extinction³⁰, and may in a multi-phage environment
171 result in altered patterns of cross-resistance evolution compared to surface-based resistance³¹.
172 The identification of the drivers and consequences of CRISPR-resistance evolution might
173 help to improve our ability to predict and manipulate the outcome of bacteria-phage
174 interactions in both natural and clinical settings.

175

- 176 1. Grissa, I., Vergnaud, G. & Pourcel, C. CRISPRcompar: a website to compare clustered
177 regularly interspaced short palindromic repeats. *Nucleic Acids Res.* **36**, 52–57 (2008).
- 178 2. Barrangou, R. *et al.* CRISPR provides acquired resistance against viruses in
179 prokaryotes. *Science* **315**, 1709–12 (2007).
- 180 3. Andersson, A. F. & Banfield, J. F. Virus population dynamics and acquired virus
181 resistance in natural microbial communities. *Science* **320**, 1047–1050 (2008).
- 182 4. Westra, E. R. *et al.* Parasite exposure drives selective evolution of constitutive versus
183 inducible defense. *Curr. Biol.* **25**, 1043–1049 (2015).
- 184 5. van Houte, S., Buckling, A. & Westra, E. R. Evolutionary ecology of prokaryotic
185 immune mechanisms. *Microbiol. Mol. Biol. Rev.* **80**, 745–763 (2016).
- 186 6. Hibbing, M. E., Fuqua, C., Parsek, M. R. & Peterson, S. B. Bacterial competition:
187 surviving and thriving in the microbial jungle. *Nat. Rev. Microbiol.* **8**, 15–25 (2010).
- 188 7. O’Toole, G. A. Cystic fibrosis airway microbiome: overturning the old, opening the
189 way for the new. *J. Bacteriol.* **200**, 1–8 (2017).
- 190 8. Folkesson, A. *et al.* Adaptation of *Pseudomonas aeruginosa* to the cystic fibrosis

- 191 airway: an evolutionary perspective. *Nat. Rev. Microbiol.* **10**, 841–51 (2012).
- 192 9. Roach, D. R. & Debarbieux, L. Phage therapy: awakening a sleeping giant. *Emerg.*
193 *Top. Life Sci.* **1**, 93–103 (2017).
- 194 10. Rossitto, M., Fiscarelli, E. V. & Rosati, P. Challenges and promises for planning future
195 clinical research into bacteriophage therapy against *Pseudomonas aeruginosa* in cystic
196 fibrosis. An argumentative review. *Front. Microbiol.* **9**, 1–16 (2018).
- 197 11. De Smet, J., Hendrix, H., Blasdel, B. G., Danis-Wlodarczyk, K. & Lavigne, R.
198 *Pseudomonas* predators: understanding and exploiting phage–host interactions. *Nat.*
199 *Rev. Microbiol.* **15**, 517–530 (2017).
- 200 12. Bondy-Denomy, J. *et al.* Prophages mediate defense against phage infection through
201 diverse mechanisms. *ISME J.* **10**, 2854–2866 (2016).
- 202 13. Harrison, F. Microbial ecology of the cystic fibrosis lung. *Microbiology* **153**, 917–923
203 (2007).
- 204 14. O’Brien, S. & Fothergill, J. L. The role of multispecies social interactions in shaping
205 *Pseudomonas aeruginosa* pathogenicity in the cystic fibrosis lung. *FEMS Microbiol.*
206 *Lett.* **364**, 1–10 (2017).
- 207 15. Bhargava, N., Sharma, P. & Capalash, N. Pyocyanin stimulates quorum sensing-
208 mediated tolerance to oxidative stress and increases persister cell populations in
209 *Acinetobacter baumannii*. *Infect. Immun.* **82**, 3417–3425 (2014).
- 210 16. Rocha, G. A. *et al.* Species distribution, sequence types and antimicrobial resistance of
211 *Acinetobacter* spp. from cystic fibrosis patients. *Epidemiol. Infect.* **146**, 524–530
212 (2018).
- 213 17. Diraviam Dinesh, S. & Diraviam Dinesh, S. Artificial sputum medium. *Protoc. Exch.*
214 4–7 (2010).
- 215 18. An, D., Danhorn, T., Fuqua, C. & Parsek, M. R. Quorum sensing and motility mediate
216 interactions between *Pseudomonas aeruginosa* and *Agrobacterium tumefaciens* in
217 biofilm cocultures. *Proc. Natl. Acad. Sci.* **103**, 3828–3833 (2006).
- 218 19. O’Toole, G. A. & Kolter, R. Flagellar and twitching motility are necessary for
219 *Pseudomonas aeruginosa* biofilm development. *Mol. Microbiol.* **30**, 295–304 (1998).
- 220 20. Laanto, E., Bamford, J. K. H., Laakso, J. & Sundberg, L. R. Phage-driven loss of
221 virulence in a fish pathogenic bacterium. *PLoS One* **7**, (2012).
- 222 21. Castillo, D., Christiansen, R. H., Dalsgaard, I., Madsen, L. & Middelboe, M.
223 Bacteriophage resistance mechanisms in the fish pathogen *Flavobacterium*
224 *psychrophilum*: Linking genomic mutations to changes in bacterial virulence factors.

- 225 *Appl. Environ. Microbiol.* **81**, 1157–1167 (2015).
- 226 22. Kavanagh, K. & Reeves, E. P. Exploiting the potential of insects for *in vivo*
227 pathogenicity testing of microbial pathogens. *FEMS Microbiol. Rev.* **28**, 101–112
228 (2004).
- 229 23. Hernandez, R. J. *et al.* Using the wax moth larva *Galleria mellonella* infection model
230 to detect emerging bacterial pathogens. *PeerJ* **6**, e6150 (2019).
- 231 24. Craig, L., Pique, M. E. & Tainer, J. A. Type IV pilus structure and bacterial
232 pathogenicity. *Nat. Rev. Microbiol.* **2**, 363–378 (2004).
- 233 25. Johnson, P. T. J., de Roode, J. C. & Fenton, A. Why infectious disease research needs
234 community ecology. *Science* **349**, 1259504–1259504 (2015).
- 235 26. Alizon, S., de Roode, J. C. & Michalakakis, Y. Multiple infections and the evolution of
236 virulence. *Ecol. Lett.* **16**, 556–567 (2013).
- 237 27. Benmayor, R., Hodgson, D. J., Perron, G. G. & Buckling, A. Host mixing and disease
238 emergence. *Curr. Biol.* **19**, 764–767 (2009).
- 239 28. Keesing, F. *et al.* Impacts of biodiversity on the emergence and transmission of
240 infectious diseases. *Nature* **468**, 647–652 (2010).
- 241 29. Chabas, H. *et al.* Evolutionary emergence of infectious diseases in heterogeneous host
242 populations. *PLOS Biol.* **16**, e2006738 (2018).
- 243 30. van Houte, S. *et al.* The diversity-generating benefits of a prokaryotic adaptive
244 immune system. *Nature* **532**, 385–388 (2016).
- 245 31. Wright, R. C. T., Friman, V. P., Smith, M. C. M. & Brockhurst, M. A. Cross-resistance
246 is modular in bacteria-phage interactions. *PLoS Biol.* **16**, e2006057 (2018).
- 247 32. Martínez-García, E., Calles, B., Arévalo-Rodríguez, M. & de Lorenzo, V. pBAM1: an
248 all-synthetic genetic tool for analysis and construction of complex bacterial
249 phenotypes. *BMC Microbiol.* **11**, 38 (2011).

250

251 **Acknowledgements** The authors thank Prof. A. Buckling for critical reading of the
252 manuscript, and Prof. JP Pirnay and D. de Vos for sharing clinical isolates of *S. aureus*, *A.*
253 *baumannii*, and *B. cenocepacia*. This work was supported by grants from the ERC (ERC-
254 STG-2016-714478 - EVOIMMECH) and the NERC (NE/M018350/1), which were awarded
255 to E.R.W.

256

257 **Author Contributions**

258 Conceptualisation: E.O.A. and E.R.W. Methodology: E.O.A., A.M.L., C.R. and E.R.W.

259 Investigation: E.O.A., E.P., I.M. Formal analysis: E.O.A., E.P., I.M., C.R. and E.R.W.
260 Writing – Original draft: E.O.A. Writing – Review and editing: E.O.A. and E.R.W. Funding
261 acquisition: E.R.W.

262

263 **Competing interests**

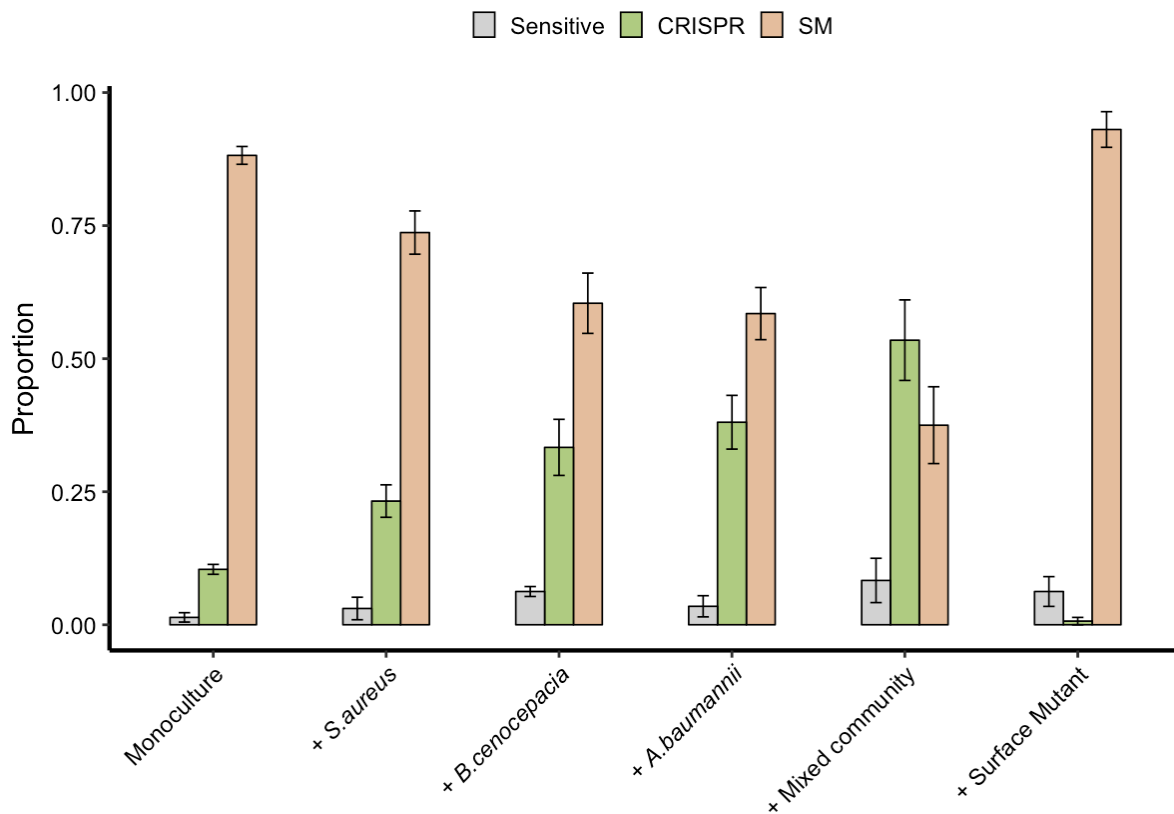
264 The authors declare no competing interests.

265 **Materials and correspondence**

266 All materials used in this study are available upon request to Edze Westra
267 (E.R.Westra@exeter.ac.uk) or Ellinor Alseth (eao210@exeter.ac.uk).

268

269

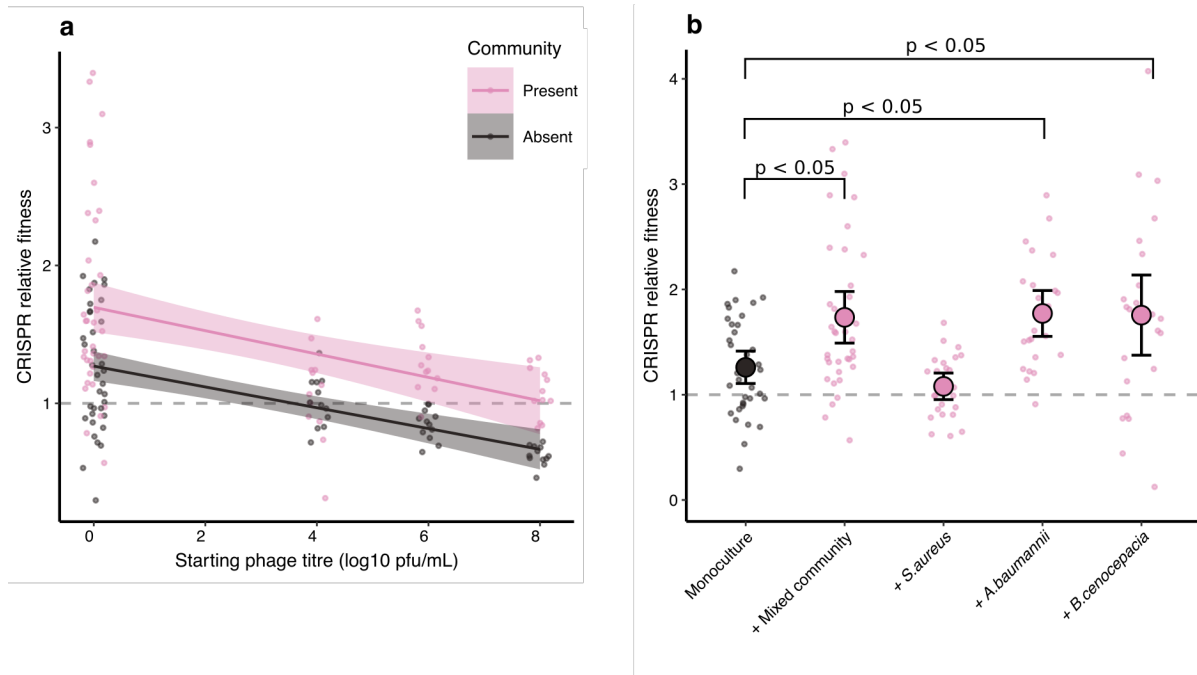


270

271 **Figure 1 | Biodiversity affects the evolution of phage resistance.** Proportion of *P.*
272 *aeruginosa* that acquired surface modification (SM) or CRISPR-based resistance, or
273 remained sensitive at 3 days post infection with phage DMS3vir (n = 6 for all treatments). *P.*
274 *aeruginosa* was grown in monoculture and in polycultures with other bacterial species
275 individually or as a mixture, or with an isogenic surface mutant. Error bars correspond to ±
276 one standard error.

277

278



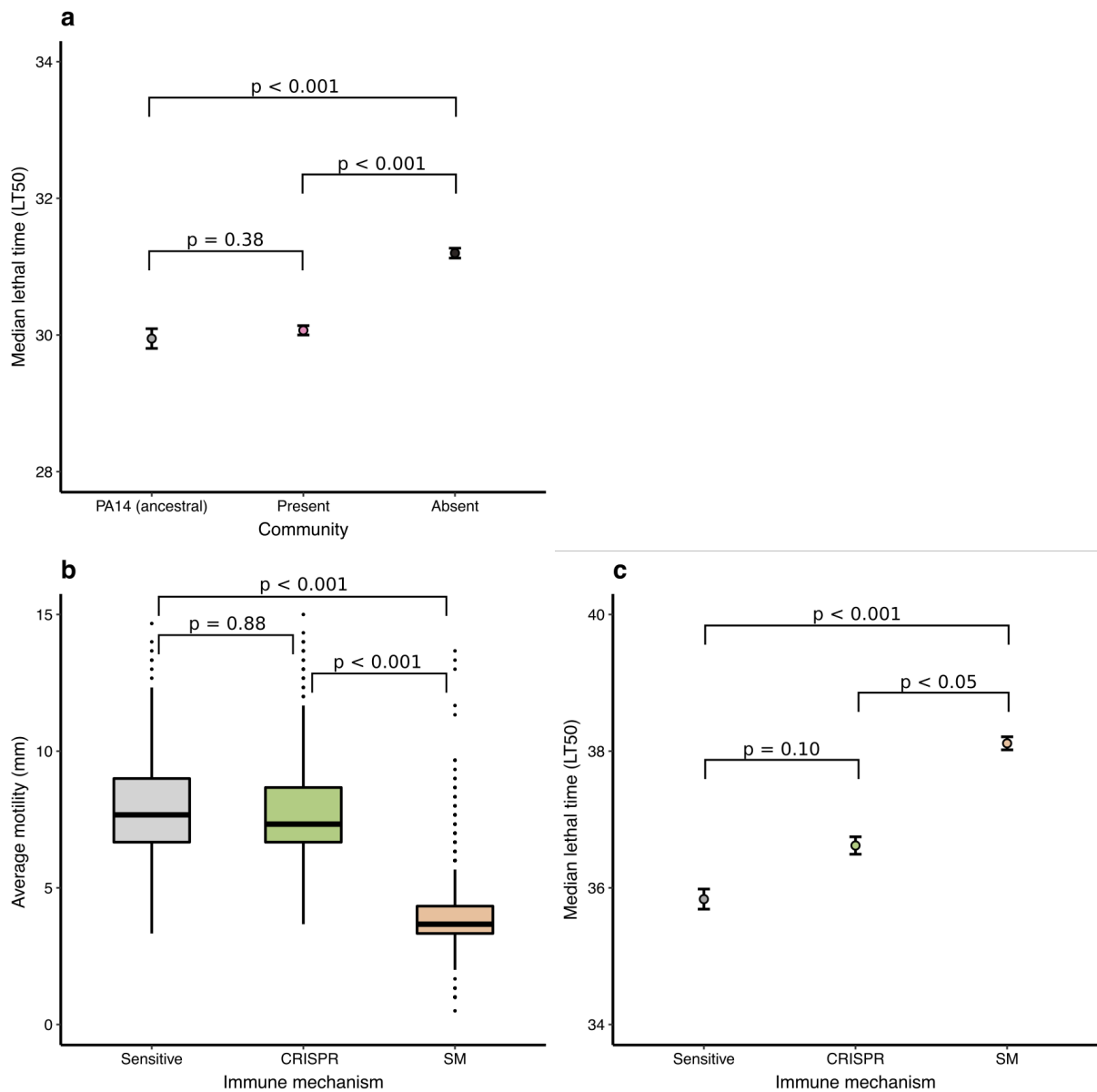
279

280 **Figure 2 | Biodiversity mitigates fitness costs associated with CRISPR-based resistance.**

281 Relative fitness of a *P. aeruginosa* clone with CRISPR-based resistance after competing for
282 one day against a surface modification clone at (a) varying levels of phage DMS3vir in the
283 presence or absence of a mixed microbial community, or (b) in absence of phage, but in the
284 presence of a mixed community or its individual bacterial species. Error bars correspond to
285 95% confidence intervals.

286

287



288

289 **Figure 3 | Evolution of phage resistance affects *in vivo* virulence.** Median lethal time
290 (LT50 = the timepoint when half of the infected larvae were dead) for (a) PA14 clones that
291 evolved phage resistance either in the presence or absence or a mixed microbial community.
292 Type of evolved phage resistance drastically impacted (b) motility, and (c) *in vivo* virulence.
293 Error bars correspond to \pm one standard error.

294

295 **Methods**

296 All statistical analyses were done using R version 3.5.1. (R Core Team, 2018), and the
297 Tidyverse package version 1.2.1. (Wickham, 2017). All *Galleria mellonella* mortality
298 analyses were done using the Survival package version 2.38 (Therneau, 2015).

299

300 **Bacterial strains and viruses.** We used a marked *P. aeruginosa* UCBPP-PA14 mutant
301 carrying a streptomycin resistant gene inserted into the genome using pBAM1³² (referred to
302 as the ancestral PA14 strain). The WT PA14 bacteriophage-insensitive mutant with 2
303 CRISPR spacers (BIM5), the surface mutant derived from the PA14 *csy3::LacZ* strain, and
304 phage DMS3*vir* and DMS3*vir* +*acrFI*(carrying an anti-CRISPR gene) have all been
305 previously described (refs. 4 and 29 and references therein). The bacteria used as the
306 microbial community were *Staphylococcus aureus* strain 13 S44 S9, *Acinetobacter*
307 *baumannii* clinical isolate FZ21 and *Burkholderia cenocepacia* J2315, were all isolated from
308 patients at Queen Astrid Military Hospital, Brussels, Belgium.

309

310 **Absorption and infection assays.** Phage infectivity against each of the bacterial species used
311 in this study was assessed by spotting serial dilutions of virus DMS3*vir* on lawns of the
312 individual community bacteria, followed by checking for any plaque formation after 24 hours
313 of growth at 37°C. Adsorption assays (as shown in Extended Data Fig. 1) were performed by
314 monitoring phage titres over time, for up to an hour (At 0, 2, 4, 6, 8, 10, 15 and 20 minutes
315 post infection for PA14, and at 0, 5, 10, 20, 40 and 60 minutes post infection for the
316 individual microbial community bacteria), after inoculating the individual bacteria in mid-log
317 phage at approximately 2×10^8 c.f.u. with phage DMS3*vir* at 2×10^6 p.f.u. (final MOI =
318 0.001). Adsorption assays were carried out in LB medium, incubated at 37°C while shaking
319 at 180 r.p.m. (three independent replicates per experiment).

320

321 **Coevolution experiments.** The streptomycin resistant ancestral strain of *P. aeruginosa* was
322 used for all coevolution experiments. The experiments (shown in Fig. 1, and Extended Data
323 Figs. 2 and 3) were performed by inoculating 60µl of approximately 10^6 colony-forming
324 units (c.f.u.) of bacteria from overnight cultures into glass microcosms containing 6ml LB
325 medium (Fig. 1 and Extended Data Fig. 3), or artificial sputum medium (for composition, see
326 ref. 17) (Extended Data Fig. 2), followed by incubation at 37°C while shaking at 180 r.p.m. (n
327 = 6 per treatment, except for Extended Data Fig. 2 monoculture in LB treatment, where n =
328 4). The polyculture mixes either consisted of approximately equal amounts of all four

329 bacterial species or mixes of *P. aeruginosa* with just one additional species where *P.*
330 *aeruginosa* made up 25% of the total volume (60 μ l). For the experiment shown in Extended
331 Data Fig. 3, *P. aeruginosa* was grown in the presence of the mixed microbial community, but
332 at a range of different starting percentages based a total volume of 60 μ l. Before inoculation,
333 phage DMS3*vir* was added at 10⁶ p.f.u. (Fig. 1), or at 10⁴ p.f.u. (Extended Data Fig. 2 and 3).
334 Transfers of 1:100 into fresh broth were done daily for a total of three days. Additionally,
335 phage titres were monitored daily by spotting chloroform-extracted phage dilutions on a lawn
336 of *P. aeruginosa* *csy3::LacZ*. Downstream analysis to determine phage resistance was done
337 using cross-streak assays and PCR as described in ref. 4.

338

339 **Competition experiments.** For both competition experiments shown in Fig. 2, the BIM5
340 clone was competed against the *csy3::LacZ* surface mutant. Bacteria were grown for 24 hours
341 in glass microcosms containing 6ml LB medium, in a shaking incubator at 180 r.p.m. and at
342 37°C. For the experiment shown in Fig. 2a, the two phenotypes were competed in the
343 presence or absence of the mixed microbial community, either without the addition of phage
344 (n = 36), or infected with phage DMS3*vir* at 10⁴, 10⁶, and 10⁸ p.f.u. (n = 12 per treatment).
345 For the experiment shown in Fig. 2b, the two phage resistant phenotypes were again
346 competed either in the presence or absence of the mixed microbial community, with the
347 addition of the individual bacterial species with the *P. aeruginosa* phenotypes always making
348 up 25% of the total volume of 60 μ l (n = 24 per treatment). Samples were taken at 0 and 24
349 hours post infection., and the cells were serial diluted in M9 salts and plated on cetrimide
350 agar (Sigma) supplemented with ca. 50 μ g ml⁻¹ X-gal (to select for *P. aeruginosa*, while also
351 differentiating between the BIM5 CRISPR clones (white) and CRISPR-KO surface mutant
352 (blue)). Relative fitness was calculated as described in refs. 4 and 29.

353

354 ***Galleria mellonella* infection experiments.** All virulence assays were done by injecting 10 μ l
355 of diluted sample into the rear proleg of individual *Galleria mellonella* larvae using a sterile
356 syringe as described in ref. 23. All larvae were checked for mortality and melanisation before
357 injection. For the experiment shown in Fig. 3a, all evolved clones from the 25% (community
358 present) and 100% (community absent) (Extended Data Fig. 3) were pooled together by
359 replica (n = 6 per treatment) in 6mL of LB medium, with ten larvae infected per replica in
360 three independent repeats (total no. of larvae = 376). To assess virulence of all evolved clones
361 (Fig. 3c), infections were done independently using all the individual PA14 clones from the
362 experiment shown in Extended Data Fig. 3, n = 981. Throughout the experiment, larvae were

363 stored in 12-well plates, with one larva per well. Prior to injection, inoculums were prepared
364 by transferring 5 μ l of all clones from the coevolution experiment to new 96-well plates
365 containing 200 μ l LB medium, before being incubated for 24h at 37°C on an orbital shaker
366 (180 r.p.m). For all experiments, after overnight growth at 37°C rotating at 180 r.p.m., the
367 bacteria were diluted by adding 20 μ l to 180 μ l of M9 salts. Cell density was then assayed by
368 measuring OD₆₀₀ absorbance, with 0.1OD being $\sim 1 \times 10^8$ cfu/ml, before being further diluted
369 down to approximately 10^4 cfu/ml, which was subsequently used for injection. Following
370 infection, larvae were incubated at 28°C, with mortality monitored hourly for up to 48 hours.
371 For both experiments, a control where larvae were injected with just M9 salts was included.

372

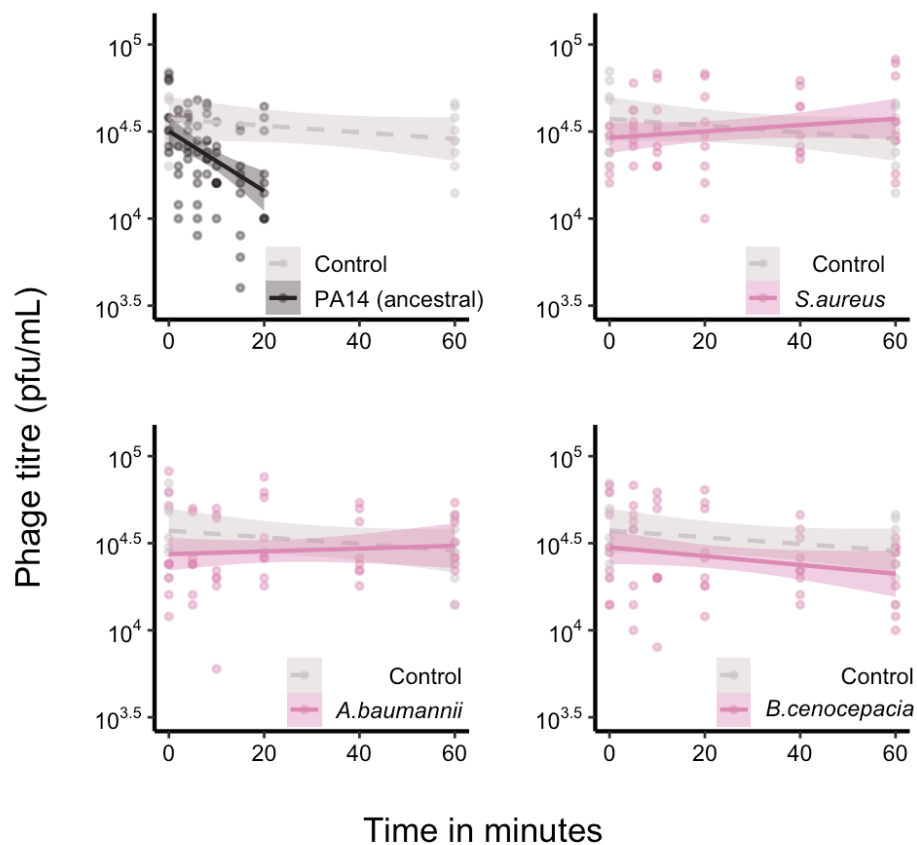
373 **Motility assays.**

374 Swarming motility of all evolved bacterial clones from the experiment shown in Extended
375 Data Fig. 3 (n = 980) was assayed by using a 96-well microplate pin replicator to stamp the
376 individual clones on 1% agar before overnight growth at 37°C. The diameters of the
377 individual clones were then taken as a measure of motility (three replicas per clone).

378

379

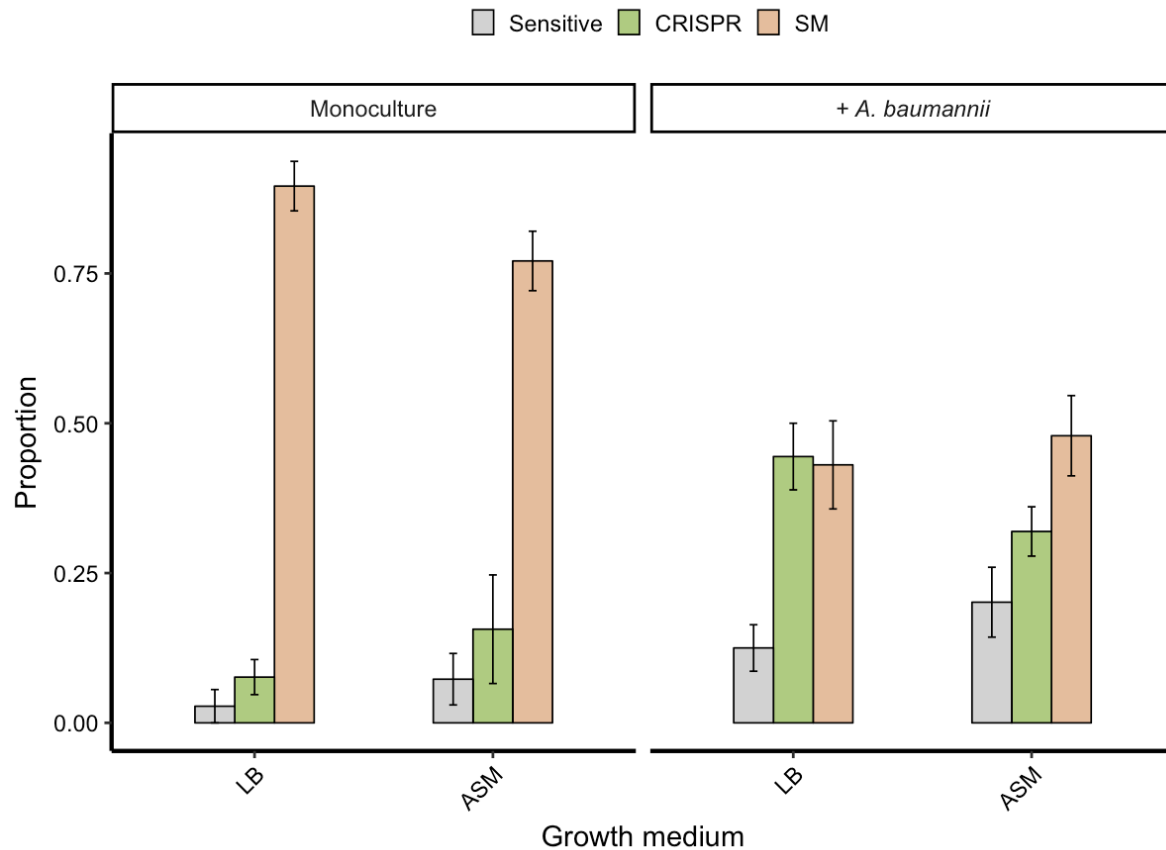
380



381

382 **Extended Data Figure 1. Only *P. aeruginosa* adsorbs phage DMS3vir.** Phage levels, given
383 in plaque-forming units per millilitre, in minutes post infection of *P. aeruginosa* PA14 and
384 three other bacterial species. Controls were carried out in the absence of bacteria. Shaded
385 areas correspond to 95% confidence intervals.

386



387

388 **Extended Data Figure 2. Enhanced CRISPR resistance evolution in artificial sputum**

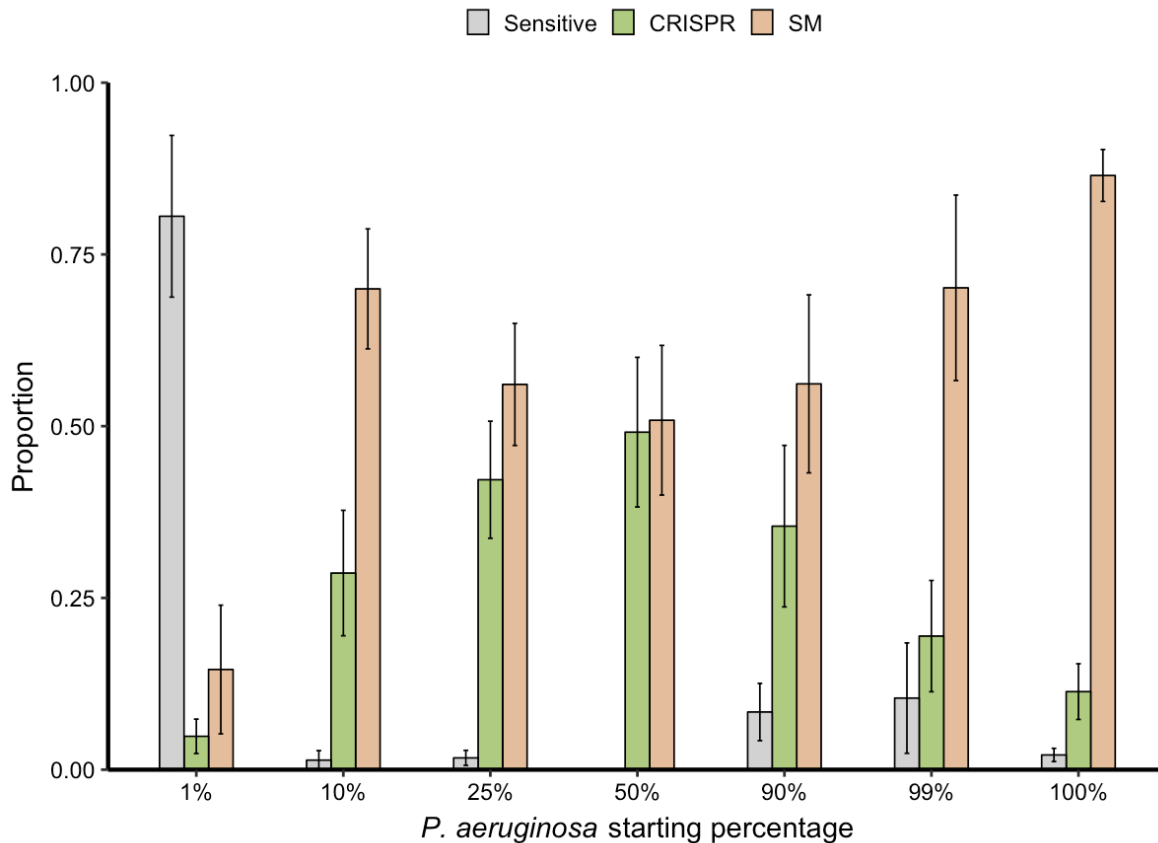
389 **medium.** Proportion of *P. aeruginosa* that acquired surface modification (SM) or CRISPR-

390 based immunity (or remained sensitive) at 3 days post infection with phage DMS3vir when

391 grown in either LB or artificial sputum medium (ASM), and in the absence or presence of *A.*

392 *baumannii*. Error bars correspond to \pm one standard error.

393



394

395 **Extended Data Figure 3. Increased CRISPR-based resistance evolution across a range**

396 **of microbial community compositions.** Proportion of *P. aeruginosa* that acquired surface

397 modification (SM) or CRISPR-based immunity (or remained sensitive) at 3 days post

398 infection with phage DMS3vir when grown either in monoculture (100%), or in polyculture

399 mixtures consisting of the mixed microbial community but with varying starting percentages

400 of *P. aeruginosa* based on volume. Error bars correspond to \pm one standard error. Deviance

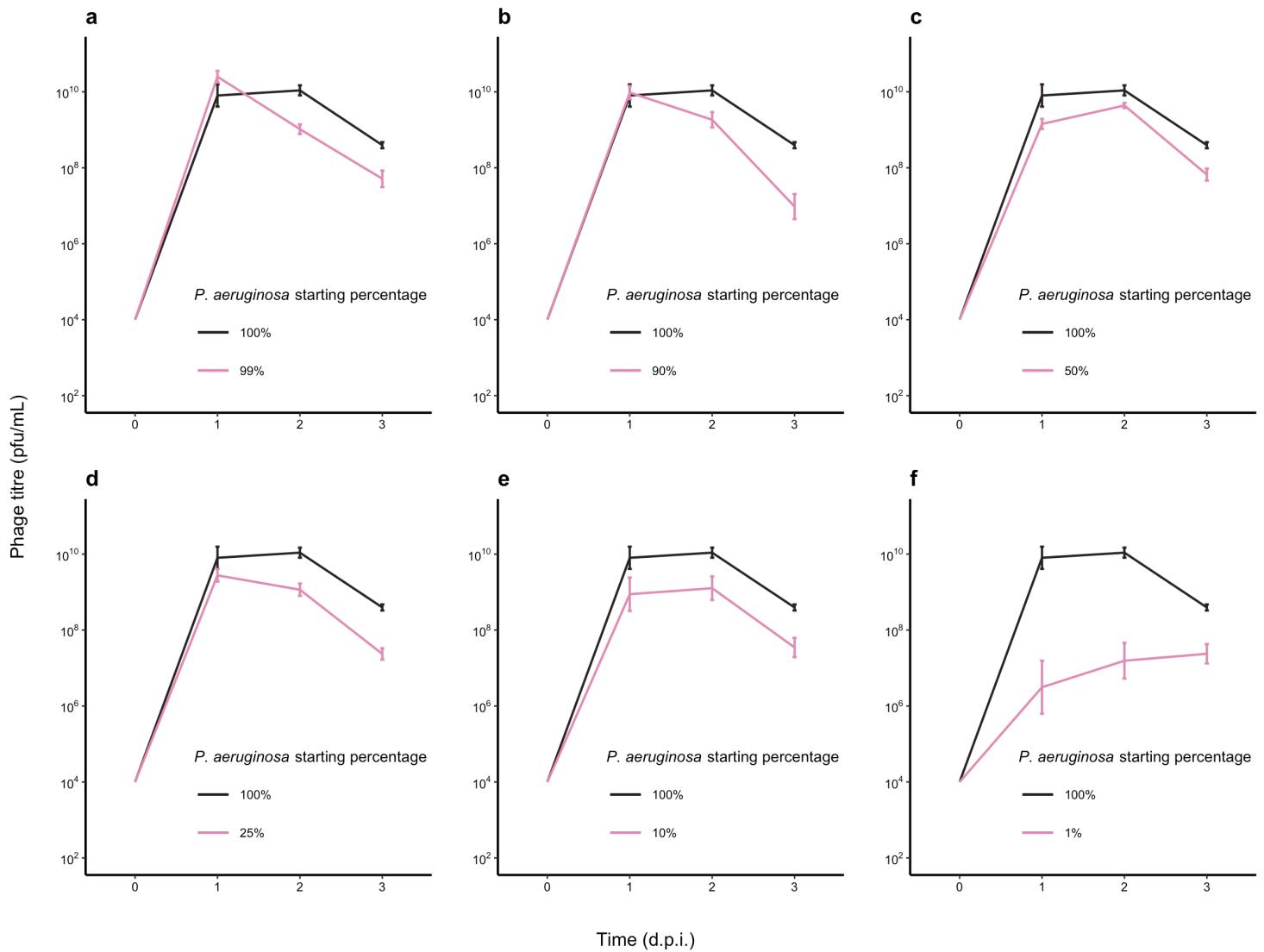
401 test: Relationship between CRISPR and *P. aeruginosa* starting percentage; Residual

402 deviance(35, n = 42) = 8.24, $p < 0.001$; 1%; $z = -3.38$, $p < 0.01$; 10%; $z = 2.12$, $p < 0.05$;

403 25%; $z = 2.77$, $p < 0.01$; 50%; $z = 3.07$, $p < 0.01$; 90%; $z = 2.46$, $p < 0.05$; 99%; $z = 1.55$, $p =$

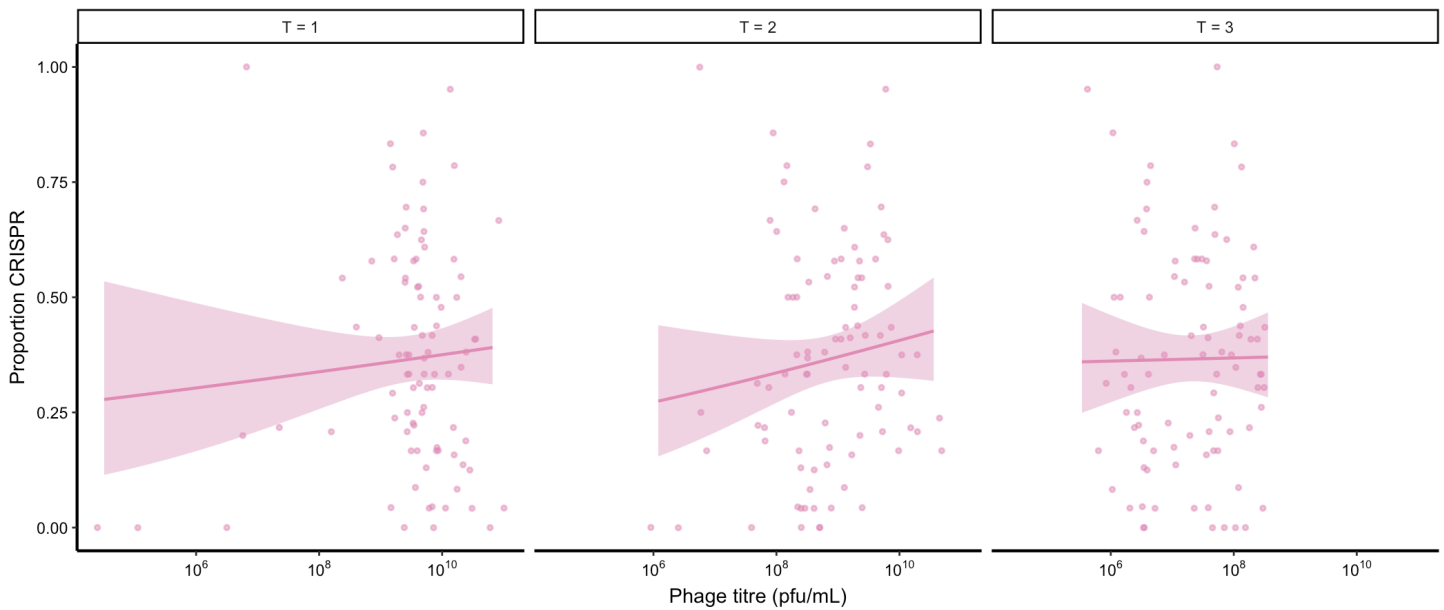
404 0.13; 100%; $z = 0.87$, $p = 0.39$.

405



406 **Extended Data Figure 4. Microbial community composition impacts phage epidemic**
407 **size.** The DMS3vir phage titres (in plaque-forming units per millilitre) over time up to 3 days
408 post infection of *P. aeruginosa* grown either in monoculture (100%), or in polyculture
409 mixtures as shown in Extended Data Fig. 3. Error bars correspond to ± one standard error.
410

411



412 **Extended Data Figure 5. No correlation between phage epidemic size and evolution of**
413 **CRISPR resistance.** The correlation between the proportion of evolved CRISPR-based
414 resistance and the phage epidemic sizes (in plaque-forming units per millilitre) using data
415 taken from experiments shown in Fig. 1, Extended Data Fig. 2 and Extended Data Fig. 3.
416 Correlations are separated by day, as phage titre was measured daily. Shaded areas
417 correspond to 95% confidence intervals. Pearson's correlations between phage titres (at each
418 day post infection) and levels of CRISPR-based resistance.: T = 1; $t_{88} = 0.75$, $p = 0.50$, $R^2 =$
419 0.08 ; T = 2; $t_{88} = 1.21$, $p = 0.23$, $R^2 = 0.13$; T = 3; $t_{88} = 0.11$, $p = 0.92$, $R^2 = 0.01$.

420